

Modeling Electron Emission from Controlled Rough Surfaces

D. A. Dimitrov
Tech-X Corporation, Boulder, CO

This work is funded by the US DoE office of Basic Energy Sciences under the SBIR grant # DE-SC0013190.

P3 Workshop, Jefferson Lab, VA, October 2016

This work was done in collaboration with:

- John Smedley and Ilan Ben-Zvi, Brookhaven National Lab.
- Howard Padmore and Siddharth Karkare, Lawrence Berkeley National Lab.
- George Bell and David Smithe, Tech-X Corp.

Outline

- 1 Motivation
- 2 Modeling
- 3 Simulations
- 4 Summary & future developments

Motivation

- Developments in materials design and synthesis have resulted in photocathodes that can have a high quantum efficiency (QE), operate at visible wavelengths, and are robust enough to operate in high electric field gradient photoguns, for application to free electron lasers and in dynamic electron microscopy and diffraction.
- However, synthesis often results in roughness, ranging from the nano to the microscale. The effect of this roughness in a high gradient accelerator is to produce a small transverse accelerating gradient, which therefore results in emittance growth.
- Although analytical formulations of the effects of roughness have been developed, detailed theoretical modeling and simulations that are verified against experimental data are lacking.
- We aim to develop realistic electron emission modeling and 3D simulations from photocathodes with controlled surface roughness to enable an efficient way to explore parameter regimes of relevant experiments.

Momentatron experiments allow investigation of emission properties and surface roughness effects.

- Recent advances in material science methods have been demonstrated (H. A. Padmore. *Measurement of the transverse momentum of electrons from a photocathode as a function of photon energy*, in P3 2014) to control the growth of photoemissive materials (e.g. Sb) on a substrate to create different types of rough layers with a variable thickness of the order of 10 nm.
- Momentatron experiments have been developed (J. Feng *et al.*, *Rev. Sc. Instr.*, **86**, 015103-1/5, 2015) to measure transverse electron momentum and emittance.
- It was demonstrated (J. Feng *et al.*, *Appl. Phys. Lett.*, **107**, 134101-1/4 2015) recently how data from momentatron experiments can be used to investigate the thermal limit of intrinsic emittance of metal photocathodes.

Momentatron concept

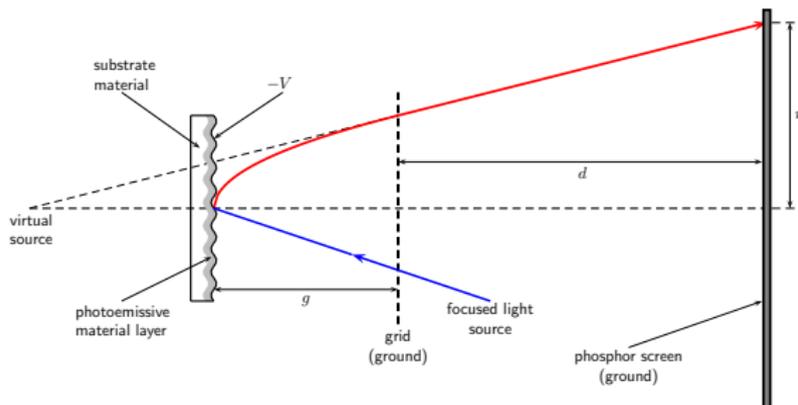


Figure 1: We have implemented some of the modeling capabilities needed and used them to simulate electron emission from rough and flat surfaces of a semimetallic (Sb) and semiconducting (GaAs) photoemissive materials.

Overview of our modeling approach

The overall modeling capabilities needed, within the Vorpal/VSim Particle-in-Cell (PIC) code framework, to simulate electron emission from photocathodes with controlled rough surfaces consist of

- electron excitation in a photoemissive material in response to absorption of photons with a given wavelength
- charge dynamics due to drift and various types of scattering processes
- representation of rough interfaces
- calculation of electron emission probabilities that takes into account image charge and field enhancement effects across rough surfaces
- particle reflection/emission updates and efficient 3D electrostatic (ES) solver for a simulation domain that has sub-domains with different dielectric properties separated by piece-wise continuous rough interfaces.

Modeling electron photo excitation

- The spatial distribution of excited electrons is modeled from an exponential decay relative to the location an absorbed photon impacts the emission surface:

$$\Delta N_{abs}^{ph}(x_i - \Delta x < x < x_i, y, z, t) \approx N_{abs}^{ph}(x = x_s, y, z, t) \frac{\exp\left(-\frac{|x_s - x_i|}{a(\hbar\omega)}\right) \Delta x}{a(\hbar\omega)}$$

- Given a laser pulse intensity profile and reflection coefficient R for the photocathode material, the number of photons absorbed through a particular photocathode surface cell with area $\Delta S = \Delta y \times \Delta z$ over the time interval from t to $t + \Delta t$ is determined from:

$$N_{abs}^{ph}(x = x_s, y, z, t) \approx (1 - R) I(x_s, y, z, t) \Delta S \Delta t / (\hbar\omega)$$

- The energy dependence of the absorption length $a(\hbar\omega)$ for ranges of interest is determined from published optical data (e.g., available for Sb in M. Cardona and D. L. Greenaway, *Phys. Rev.* **133**, A1685 1964 and for GaAs in S. Karkare *et al.*, *J. Appl. Phys.*, **113**, 104904-1/12, 2013).

Energy and momentum of photo-excited electrons

- The energies of photo-excited electrons can be determined accurately if the band structure is known (e.g., as in GaAs).
- Another approach is to draw a sample sing a distribution determined from a density-of-states (DOS) and the Fermi-Dirac function. For the Sb simulations here, we used this approach.
- The momentum direction of a photo-excited electron is sampled from a uniform distribution on the unit sphere.

We have developed simulations with different types of surface roughness.

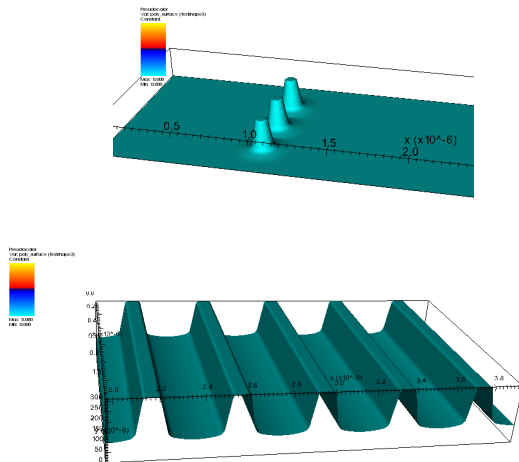


Figure 2: The surfaces are represented with cut-cell grid boundaries.

Why modeling electron-electron scattering in metals is important?

- Charged carrier-carrier binary scattering is the most important process that affects electron emission from metallic photocathodes.
- A photo-excited electron with energy higher than the work function (of the order of 1 eV) is likely to be emitted only if it does not scatter with another electron before its emission occurs.
- A single electron-electron scattering event usually reduces the energy of a photo-excited electron to practically prevent it from being emitted.
- Electron-phonon scattering has a maximum energy exchange given by the maximum optical phonon energy of around 0.1 eV.
- Many electron-phonon scattering events (phonon emission) are needed to relax the energy of a photo-excited electron to prevent it from emission.

Different approaches have been proposed to model charged carrier-carrier (binary) scattering in Monte Carlo simulations.

- In semiconductors, an approach proposed by [Lugli and Ferry, Physica 117B, 251 \(1983\)](#), can also be applied to model transient behavior ([Osman and Ferry, Phys. Rev. B, 36, 6018 \(1987\)](#)). It was later improved ([M. Moško and A. Mošková, Phys. Rev., 44 10794 \(1991\)](#)) to prevent extra energy dissipation in the original algorithm.

$$\Gamma_{eh}(\mathbf{k}_0) = \frac{p\mu e^4}{2\pi\epsilon^2\hbar^3} \int d^3k f_h(k) \frac{Q_{eh}}{\beta^2(Q_{eh}^2 + \beta^2)}$$

and

$$\Gamma_{he}(\mathbf{k}_0) = \frac{n\mu e^4}{2\pi\epsilon^2\hbar^3} \int d^3k f_e(k) \frac{Q_{he}}{\beta^2(Q_{he}^2 + \beta^2)},$$

where

$$Q_{eh} = 2\mu |\mathbf{k}_0/m_e - \mathbf{k}/m_h|, \quad Q_{he} = 2\mu |\mathbf{k}_0/m_h - \mathbf{k}/m_e|$$

$$\Gamma_{eh}(\mathbf{k}_0) = \frac{p\mu e^4}{2\pi\epsilon^2\hbar^3} \frac{1}{N_h} \sum_{\text{holes}} \frac{Q_{eh}}{\beta^2(Q_{eh}^2 + \beta^2)} \quad (10)$$

and

$$\Gamma_{eh}(\mathbf{k}_0) = \frac{n\mu e^4}{2\pi\epsilon^2\hbar^3} \frac{1}{N_e} \sum_{\text{electrons}} \frac{Q_{he}}{\beta^2(Q_{he}^2 + \beta^2)}. \quad (11)$$

To obtain the expression for the e - e scattering rate $\Gamma_{ee}(\mathbf{k}_0)$, we set $m_e = m = m_h$ and $\mu = m/2$ in (10) (choosing the appropriate mass for the electrons and conversely for the holes in h - h scattering), and

$$\Gamma_{ee}(\mathbf{k}_0) = \frac{nme^4}{4\pi\epsilon^2\hbar^3} \frac{1}{N_e} \sum_{\mathbf{k}} \frac{|\mathbf{k}_0 - \mathbf{k}|}{\beta^2(|\mathbf{k}_0 - \mathbf{k}|^2 + \beta^2)}, \quad (12)$$

- This approach is inefficient for degenerate semiconductors since the Pauli exclusion principle is applied at the end of each scattering event effectively throwing away many computations when the final states are not allowed.

We implemented a unified model for carrier-carrier scattering.

- For metals, the often used approach is based on a many-body formalism using the imaginary part of the electron self-energy.
- A Fermi golden rule approach using a screen Coulomb potential has also been used. Both approaches are complex and computationally intensive to implement in particle Monte Carlo simulations.
- Ziaja *et al.* *J. Appl. Phys.*, **99** 033514 (2006) proposed a unified model for calculation of electron-electron mean free paths (MFP) in metals and semiconductors that is applicable over a wide range of energies and is efficient for use in Monte Carlo transport simulations.
- The MFP is given (in Å) by the simple formula:

$$\lambda(E) = \frac{\sqrt{E}}{a(E - E_{th})^b} + \frac{E - E_0 \exp(-B/A)}{A \ln(E/E_0) + B},$$

where E_{th} is a threshold energy for the scattering ($E_{th} = 0$ for metals and $E_{th} = E_G$ for semiconductors), $E_0 = 1$ eV, and a , b , A , and B are fitting constants.

Scattering rates in metals could vary over several orders of magnitude in the low energy regime.

- The fitting parameters in the model are determined from experimental data (when available) and/or full band structure calculations.
- The scattering rates can be calculated from the MFP.

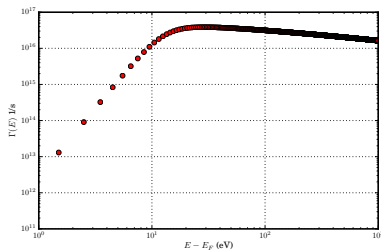
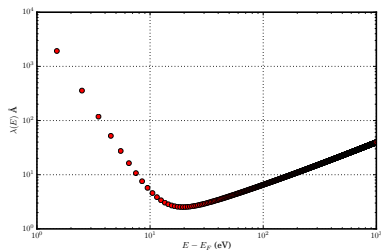


Figure 3: MFP and scattering rates determined from the unified model with the parameters for Li.

We used two sets of rates for electron-electron scattering in Sb.

- The fitting parameters are not known for Sb.
- We investigated two regimes for the rates in Sb by using low and high rates observed in some metals.

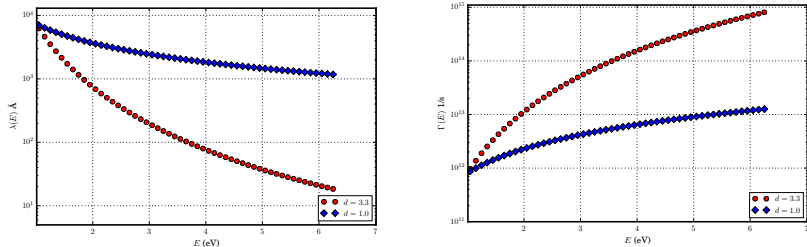


Figure 4: The two regimes of low and high MFPs (and their corresponding scattering rates) used in the simulation are plotted over a low energy range relevant to photo-excitation in emission experiments (also within the low energy regime of the scattering model: $E < E_P$ with E_P the plasmon energy).

Field enhancement on rough surfaces affects electron emission

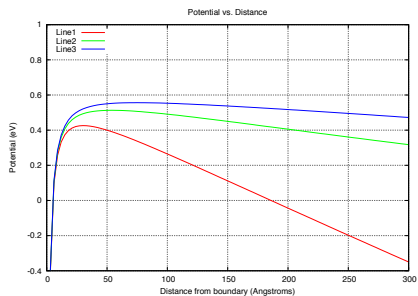
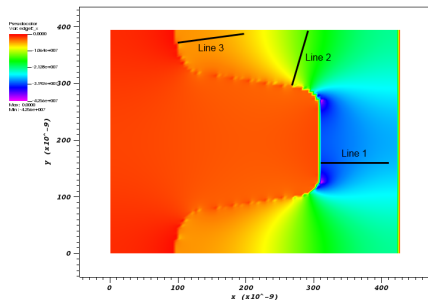


Figure 5: Longitudinal electric field (left plot) from Vorpil's ES solver for the case of a single ridge rough surface confirms the strongest field enhancement is close to the tips of the ridge. The lines shown are normal to the ridge surface at the corresponding locations. The right plot shows the surface potential energy (with $\chi = 0.63$ eV) lowering along the three lines.

Transfer matrix (TM) approach

- The emission probability is calculated by solving a 1D quantum mechanical problem with a space-varying electron mass.

General form of the 1D Schrödinger equation.

$$-\frac{\hbar^2}{2} \frac{d}{dz} \frac{1}{m^*(z)} \frac{d\psi(z)}{dz} + V_{ss}(z) \psi(z) = E_{inc} \psi(z), \quad (1)$$

- $V_{ss}(x)$ is a stair-step representation of the actual potential energy $V(x)$ across the interface.
- The energy is given by

$$E_{inc} = E_{tot} - E(k_{\perp}) = E_{tot} - \frac{(\hbar k_{\perp})^2}{2m_e},$$

where E_{tot} is the electron's total energy in diamond (before emission) and $E(k_{\perp})$ is the part of the electron's energy (in vacuum) that depends on the electron's full transverse crystal momentum k_{\perp} .

The TM method approximates a generally-shaped potential with a stair step representation.

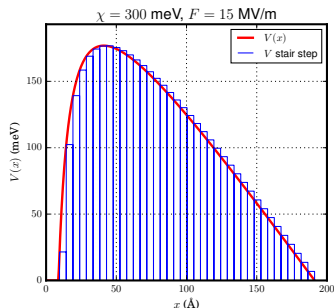


Figure 6: Example discretization of the $V(x_n) = \chi - F_n x_n - Q/x_n$ potential using ≈ 40 steps; 500 steps are used in the simulations. For metals, the electron affinity is $\chi = \mu + \Phi$, with μ the chemical potential and Φ the work function. Positions x_n and field values F_n are along emission surface outward normal directions with local origin at where particle attempted emission position. In each interval, the electron potential and its mass are considered constant but can vary from interval to interval.

Transmission probability formalism

- The transmission probability (coefficient) is defined as the ratio of the incident to transmitted current densities:

$$T(E_{inc}, k_{inc,||}) = \frac{J_{tr}(m_{tr}, k_{tr,||})}{J_{inc}(m_{inc}, k_{inc,||})}. \quad (2)$$

- The current density is determined from the solution of the Schrödinger equation:

$$J(m, k) = \frac{\hbar}{2mi} (\psi_k^*(z) \partial_z \psi_k(z) - \psi_k(z) \partial_z \psi_k^*(z)).$$

- In the transfer matrix the wave functions are plane waves in each of the intervals with a constant potential energy.

Simulations of emission from a grated ridge confirm the expected effect of field enhancement.

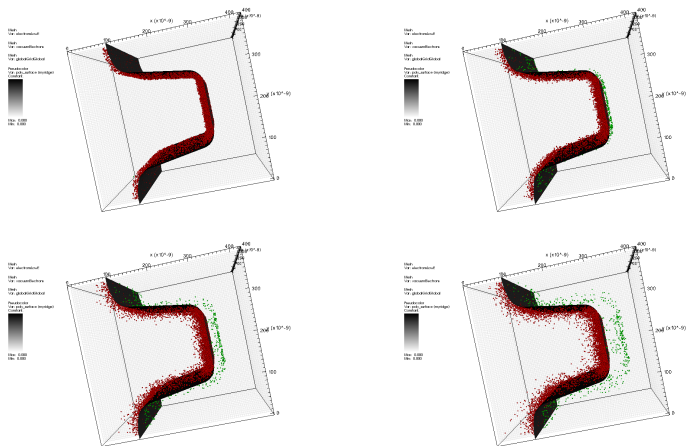


Figure 7: Particles loaded manually within a 20 nm distance from the emission surface assuming light impacting the ridge surface along the negative x axis. GaAs is used for modeling electron drift/diffusion in the photocathode material.

We compare results from simulations with flat and 3-ridge rough emission surfaces.

- We did initial development using a GaAs emission layer.
- Recently, simulations were extended to Sb (work function of 4.4 eV) with only electron-electron scattering included.
- A constant potential difference is maintained across the x length of the simulation domain leading to an applied field magnitude in the vacuum region of the order of 1 MV/m (it varies on the rough emission surface).
- The controlled rough surface has a ridge period of 394 nm, ridge height of 194 nm, and a width of the ridge flat top of 79 nm - based on grated surfaces grown in LBNL (data provided by H. Padmore).
- We use periodic boundary conditions in the transverse directions.
- The simulation domain size for both the 3-ridge and the flat emission surfaces is $0.4268 \times 1.182 \times 0.394$, in μm , with $88 \times 264 \times 16$ number of cells. The time step was 2.5×10^{-16} s.

Photo-excited electrons are loaded in a surface layer with 20 nm width.

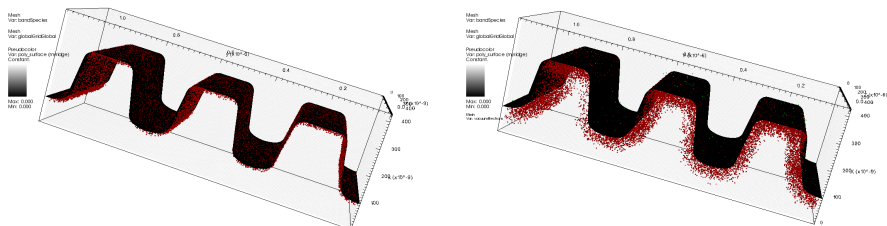


Figure 8: Electrons are initialized only at $t = 0$ s (left plot) in the photocathode material sub-domain of the simulation (shown with red spheres). The electron dynamics in Sb is practically diffusive with only a small number emitted into the vacuum sub-domain, shown with green spheres in the right plot at simulation time of 25 fs.

The simulations are started with 30k photo-excited electrons

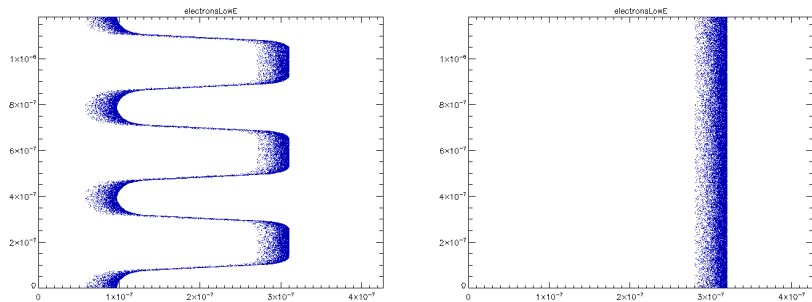


Figure 9: A sample distribution of loaded electrons projected to the y-z plane.

Typical patterns of field enhancement on the rough and flat emission surfaces used in the simulations.

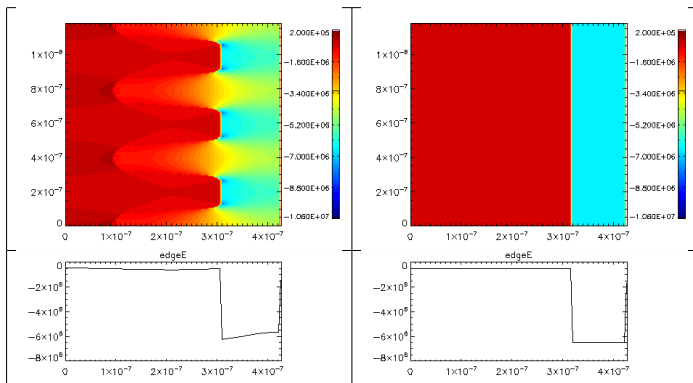
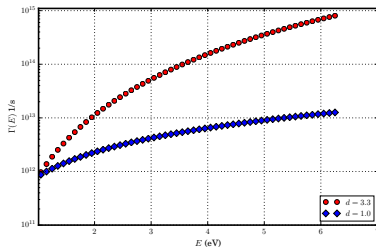
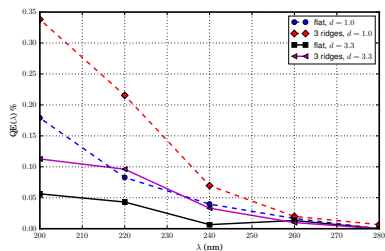


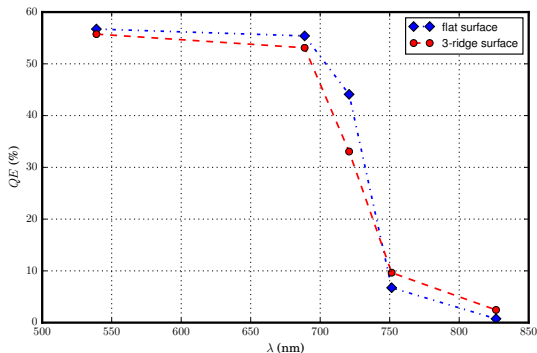
Figure 10: E_x component of the electric field calculated from the ES solver. Intensity in the x - y plane and a line-out at $y = L_y/2$. The field due to space charge is not taken into account.

Effects of roughness and electron-electron scattering on quantum efficiency in simulations for Sb.



- For the same scattering rates, the field enhancement on the rough surface leads to higher QE than from the flat one.
- Increase of scattering rates by an order of magnitude caused a decrease in the QE by a factor of around two - it is also photon energy dependent.
- The energy dependence of the scattering rate affects the spectral response of the QE.

QE in GaAs is less affected by this type of roughness.



- The electron dynamics is very different. In Sb, the dynamics is diffusion dominated. In GaAs, it involves both drift and diffusion.
- The simulations were done with electron affinity set to 0.3 eV for increased emission.

The roughness causes greater deviations in the mean transverse energy (MTE).

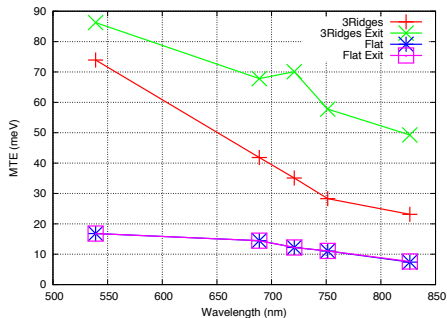


Figure 11: Comparison of MTE results from the flat and 3-ridges emission surfaces for the photon wavelengths simulated. The results are calculated at the emission surface and at a diagnostics surface near the exit of the simulation domain.

- The MTE for the flat emission surface does not depend on where we calculate the MTE since the electric field does not have non-zero transverse components in vacuum.

Roughness causes a tail in the angular distribution of emitted electrons.

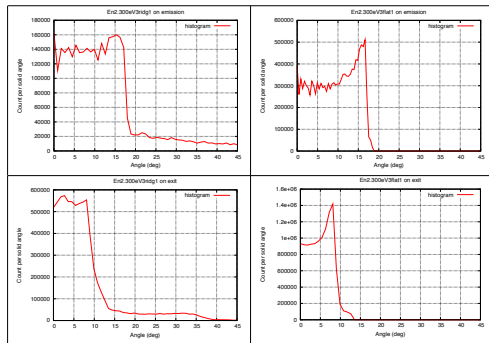


Figure 12: Photon energy was $\hbar\omega = 2.3$ eV. Left column is from the the 3-ridge emission surface runs and the right column is from the flat surface ones. Top row is for the distribution at the emission surface while the bottom row is for the diagnostics surface near the exit of the simulation domain. The tail is likely due to transverse field components between the ridges and emission from the ridge walls and the valleys.

Summary

- We implemented models to simulate electron emission from Sb and GaAs photocathodes with controlled rough surfaces in the 3D VSim PIC code.
- Initial results show that the QE from rough Sb surfaces was higher than from flat ones. This behavior is reversed when using GaAs. However, the electron dynamics in GaAs has a strong drift component compared to Sb which is diffusion dominated. In GaAs, scattering is mainly with low-energy phonon processes allowing electrons to survive for much longer time also leading to much higher QE values.
- Transverse fields in the regions between ridges could lead to increase of the MTE by a factor of two or more.
- Future work will include accurate representation of the DOS (Bullett, 1975), modeling time-varying laser pulse absorption at oblique incidence, surface-varying (due to interference) light intensity absorption, and finite emissive layer thickness modeling.

Acknowledgements

We would like to acknowledge helpful discussions on the physics of photocathodes with:

- Erdong Wang, Erik Muller, Mengjia Gaowei, and Triveni Rao, BNL.
- Ivan Bazarov, Cornell University.
- Kevin Jensen, NRL.
- Members of the Vorpal/VSim code development team and particularly John R. Cary and Sean Zhu.

We are grateful to the DoE office of Basic Energy Sciences for funding this work.

Field enhancement effects in GaAs Simulations with rough surfaces.

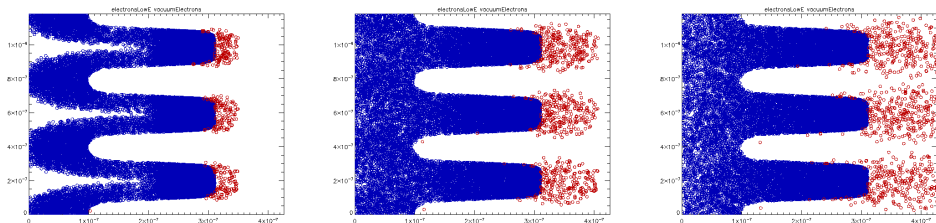


Figure 13: Electron emission at times 0.125 ps, 0.25 ps, and 0.325 ps for photon energy of 1.65 eV. Electrons in GaAs are plotted with blue circles while vacuum electrons are plotted with red ones.